The Autism-Related Protein CHD8 Cooperates with C/EBPβ to Regulate Adipogenesis

喜多, 泰之

Article

Cell Reports

The Autism-Related Protein CHD8 Cooperates with C/EBPβ to Regulate Adipogenesis

Graphical Abstract

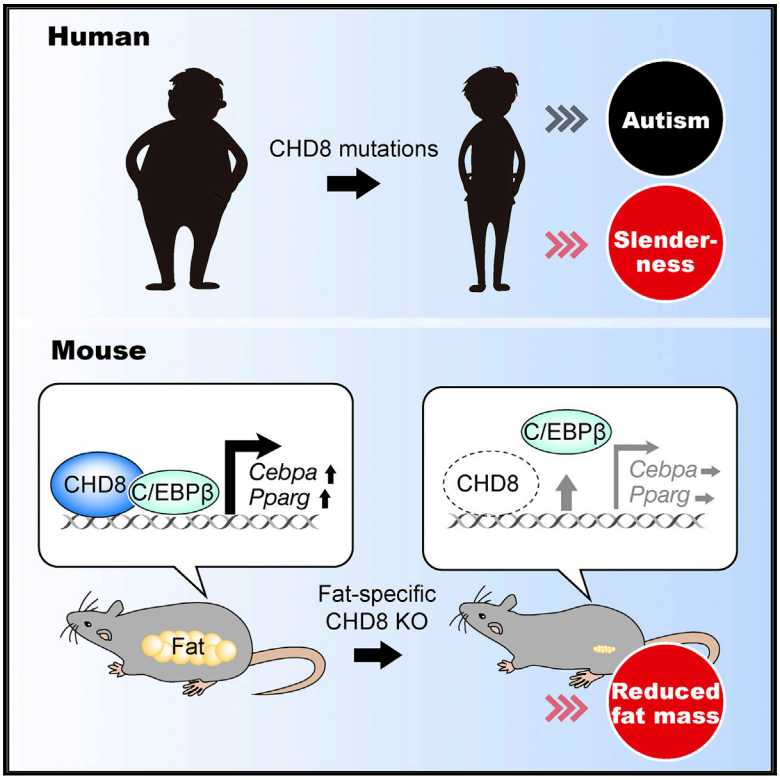

Highlights

- CHD8 directly regulates C/EBPα and PPARγ during adipogenesis
- CHD8 interacts with C/EBPβ and promotes its transactivity
- CHD8 ablation in preadipocytes results in a markedly reduced fat mass
- CHD8 is essential for not only neuronal development but also adipose development

Authors

Yasuyuki Kita, Yuta Katayama, Taichi Shiraishi, ..., Michiko Shirane, Masaaki Nishiyama, Keiichi I. Nakayama

Correspondence

nishiyam@staff.kanazawa-u.ac.jp (M.N.), nakayak1@bioreg.kyushu-u.ac.jp (K.I.N.)

In Brief

Kita et al. show that autism-related protein CHD8 is essential for adipogenesis and the development of white adipose tissue. Moreover, they demonstrate that CHD8 cooperates with C/EBPβ to regulate transactivation of the genes for C/EBPα and PPARγ during adipogenesis.

Kita et al., 2018, Cell Reports *23*, 1988–2000
May 15, 2018
https://doi.org/10.1016/j.celrep.2018.04.050

CellPress

OPEN ACCESS
CellPress

Cell Reports
Article

The Autism-Related Protein CHD8 Cooperates with C/EBPβ to Regulate Adipogenesis

Yasuyuki Kita,[1,2] Yuta Katayama,[1] Taichi Shiraishi,[1] Takeru Oka,[1] Tetsuya Sato,[3] Mikita Suyama,[3] Yasuyuki Ohkawa,[4] Keishi Miyata,[5] Yuichi Oike,[5] Michiko Shirane,[1,2] Masaaki Nishiyama,[1,6,*] and Keiichi I. Nakayama[1,7,*]

[1]Department of Molecular and Cellular Biology, Medical Institute of Bioregulation, Kyushu University, 3-1-1 Maidashi, Higashi-ku, Fukuoka, Fukuoka 812-8582, Japan

[2]Department of Molecular Biology, Graduate School of Pharmaceutical Sciences, Nagoya City University, 3-1 Tanabe-dori, Mizuho-ku, Nagoya, Aichi 467-8603, Japan

[3]Division of Bioinformatics, Medical Institute of Bioregulation, Kyushu University, 3-1-1 Maidashi, Higashi-ku, Fukuoka, Fukuoka 812-8582, Japan

[4]Division of Transcriptomics, Medical Institute of Bioregulation, Kyushu University, 3-1-1 Maidashi, Higashi-ku, Fukuoka, Fukuoka 812-8582, Japan

[5]Department of Molecular Genetics, Graduate School of Medical Sciences, Kumamoto University, 1-1-1 Honjo, Chuo-ku, Kumamoto 860-8556, Japan

[6]Department of Histology and Cell Biology, Graduate School of Medical Sciences, Kanazawa University, 13-1 Takaramachi, Kanazawa, Ishikawa 920-8640, Japan

[7]Lead Contact

*Correspondence: nishiyam@staff.kanazawa-u.ac.jp (M.N.), nakayak1@bioreg.kyushu-u.ac.jp (K.I.N.)

https://doi.org/10.1016/j.celrep.2018.04.050

SUMMARY

The gene encoding the chromatin remodeler CHD8 is the most frequently mutated gene in individuals with autism spectrum disorder (ASD). Heterozygous mutations in *CHD8* give rise to ASD that is often accompanied by macrocephaly, gastrointestinal complaints, and slender habitus. Whereas most phenotypes of CHD8 haploinsufficiency likely result from delayed neurodevelopment, the mechanism underlying slender habitus has remained unknown. Here, we show that CHD8 interacts with CCAAT/enhancer-binding protein β (C/EBPβ) and promotes its transactivation activity during adipocyte differentiation. Adipogenesis was impaired in *Chd8*-deleted preadipocytes, with the upregulation of C/EBPα and peroxisome-proliferator-activated receptor γ (PPARγ), two master regulators of this process, being attenuated in mutant cells. Furthermore, mice with CHD8 ablation in white preadipocytes had a markedly reduced white adipose tissue mass. Our findings reveal a mode of C/EBPβ regulation by CHD8 during adipogenesis, with CHD8 deficiency resulting in a defect in the development of white adipose tissue.

INTRODUCTION

Autism spectrum disorder (ASD) is a neurodevelopmental disorder with a high prevalence (~2% of the global population) (Schaaf and Zoghbi, 2011; Taylor et al., 2013). Recent exome-sequencing studies of individuals with ASD have identified many mutations, with the gene encoding the chromatin remodeler CHD8 (chromodomain helicase DNA-binding protein 8) being the most frequent site of such mutations (Neale et al., 2012; O'Roak et al., 2012a, 2012b; Talkowski et al., 2012). Many studies of CHD8 have thus focused on its role in neurogenesis and brain development (Cotney et al., 2015; Sugathan et al., 2014). CHD8 is expressed not only in neuronal tissues but also in many other organs, where it may also play an important developmental role (Ishihara et al., 2006; Nishiyama et al., 2009). Indeed, individuals with *CHD8* mutations manifest not only ASD but also macrocephaly, distinct facial characteristics, gastrointestinal complaints, and a tall and slender habitus. Although psychological symptoms, macrocephaly, and gastrointestinal complaints resulting from CHD8 haploinsufficiency are likely attributable to defective neuronal development and associated responses, the mechanism by which *CHD8* mutations give rise to slenderness has remained unclear (Bernier et al., 2014; Katayama et al., 2016). Such slenderness is an unexpected characteristic, given that ASD patients in general tend to be obese as a result of food selectivity, gastrointestinal symptoms, reduced physical activity, and medication use (Curtin et al., 2010, 2014; Zheng et al., 2017). These observations suggest that CHD8 might also contribute to regulation of metabolism or adipogenesis.

CHD8 is a member of the CHD family of enzymes that belong to the SNF2 superfamily of ATP-dependent chromatin remodelers and are defined by the presence of two chromodomains: a helicase/ATPase domain and a DNA-binding domain (Hall and Georgel, 2007; Marfella and Imbalzano, 2007). Several members of this family play important roles during development and are implicated in various human diseases (Ho and Crabtree, 2010). For example, CHD1 is thought to contribute to the pluripotency of embryonic stem cells by maintaining an open chromatin state (Gaspar-Maia et al., 2009). Similarly, CHD5 is a key regulator of neurogenesis and plays a dual role in the activation of neuronal genes and the repression of Polycomb target genes (Egan et al., 2013). The *CHD5* gene resides within a region of human chromosome 1p36 that shows loss of

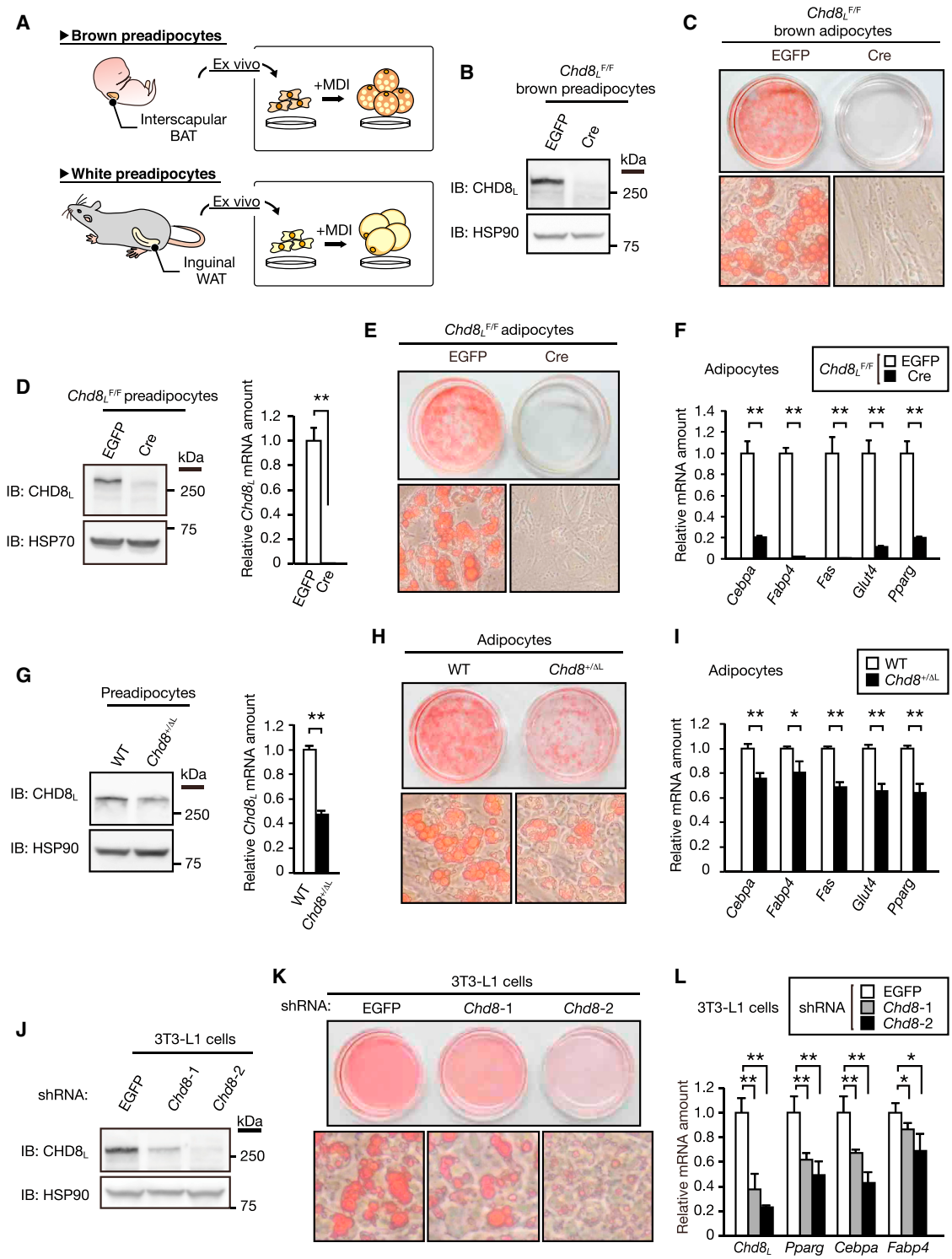

Figure 1. CHD8 Is Essential for Adipogenesis

(A) Establishment of immortalized preadipocyte lines from iWAT of 4-week-old mice and interscapular BAT of 2-day-old mice homozygous for a floxed (F) allele of *Chd8* (*Chd8*$_L^{F/F}$).

(B) Immunoblot (IB) analysis of CHD8 and HSP90 (loading control) in brown preadipocytes derived from *Chd8*$_L^{F/F}$ mice and infected with retroviruses encoding Cre or EGFP.

(C) *Chd8*$_L^{F/F}$ brown preadipocytes infected with retroviruses encoding Cre or EGFP were induced to undergo adipogenesis for 8 days and then stained with oil red O.

(legend continued on next page)

heterozygosity in individuals at high risk for the development of neuroblastoma (Bagchi et al., 2007). CHD7 is also required for neurogenesis and neural crest formation as a result of its direct binding to promoter or enhancer regions of fate-controlling transcription factor genes and consequent opening of chromatin structure (Bajpai et al., 2010; Feng et al., 2013). De novo mutations of human *CHD7* give rise to CHARGE syndrome, a condition characterized by malformation of various organs (Vissers et al., 2004).

CHD8 was originally identified as a negative regulator of the Wnt/β-catenin signaling pathway (Nishiyama et al., 2012; Sakamoto et al., 2000). *CHD8* generates two alternatively spliced transcripts that encode a 280-kDa full-length protein ($CHD8_L$) or a 110-kDa protein ($CHD8_S$) that contains only the NH_2-terminal chromodomain (Ishihara et al., 2006; Nishiyama et al., 2009). Mutations identified in individuals with ASD are distributed throughout the *CHD8* locus, with some expected to result in the loss of both CHD8 isoforms and others to affect only $CHD8_L$. To recapitulate this situation, we generated two independent lines of mutant mice deficient in both CHD8 isoforms (ΔSL) or only $CHD8_L$ (ΔL), and we found that both heterozygous mutant strains manifest ASD-like behavioral characteristics (Katayama et al., 2016). CHD8 was also shown to regulate the expression of ASD-related neurodevelopmental genes in neurons, especially those targeted by RE1-silencing transcription factor (REST), which suppresses the transcription of many neuronal genes during development.

Adipogenesis is the strictly controlled cellular process by which preadipocytes differentiate into mature adipocytes. The expression of preadipogenic transcription factors such as CCAAT/enhancer-binding protein β (C/EBPβ) and C/EBPδ is induced during the early phase of adipogenesis and is followed by that of C/EBPα and peroxisome-proliferator-activated receptor γ (PPARγ), both of which are master regulators of adipogenesis. C/EBPα and PPARγ activate the expression of multiple adipogenic genes whose products mediate the final maturation process (Siersbæk et al., 2012). In response to adipogenic stimulation, chromatin structure undergoes substantial remodeling, resulting in the activation of a complex network of these transcription factors (Rosen and MacDougald, 2006). The mechanistic basis of such chromatin remodeling during adipogenesis has remained largely unknown, however.

We now show that CHD8 is essential for adipogenesis and the development of white adipose tissue (WAT). We found that CHD8 cooperates with C/EBPβ to regulate transactivation of the genes for C/EBPα and PPARγ during adipogenesis. Generation of mice in which *Chd8* is deleted specifically in mesenchymal stem cells revealed that these animals have a markedly reduced adipose tissue mass. Our results thus indicate that CHD8 plays an essential role not only in neuronal development but also in adipogenesis.

RESULTS

CHD8 Is Required for Adipogenesis

To investigate the role of CHD8 during adipogenesis, we established immortalized $Chd8_L^{F/F}$ preadipocyte lines from inguinal WAT (iWAT) of 4-week-old mice and interscapular brown adipose tissue (BAT) of 2-day-old mice that were homozygous for a floxed (F) allele of *Chd8* (Figure 1A). The cells were infected with a retrovirus encoding Cre recombinase to generate $Chd8_L^{-/-}$ preadipocytes or with a control retrovirus encoding EGFP. We confirmed that Cre inactivated almost all floxed alleles in $Chd8_L^{F/F}$ preadipocytes (Figures 1B and 1D). Ablation of *Chd8* in preadipocytes resulted in a pronounced defect in adipogenesis in response to treatment with the combination of 3-isobutyl-1-methylxanthine, dexamethasone, and insulin (MDI) (Figures 1C and 1E). Consistent with this impairment of adipogenesis, RT-PCR and real-time PCR analysis showed that the induction of adipogenic marker genes such as *Cebpa*, *Fabp4*, *Fas*, *Glut4*, and *Pparg* was significantly attenuated in CHD8-deficient cells (Figure 1F). We also isolated preadipocytes from iWAT of wild-type (WT) or *Chd8* heterozygous mutant ($Chd8^{+/\Delta L}$) mice (Katayama et al., 2016) (Figure 1G). Exposure of these cells to MDI revealed that the ability of $Chd8^{+/\Delta L}$ preadipocytes to undergo adipogenic differentiation was impaired compared with that of WT cells (Figure 1H). The induction of adipogenic marker genes was also attenuated in $Chd8^{+/\Delta L}$ cells compared with WT cells (Figure 1I). Furthermore, we examined the effect of short hairpin RNA (shRNA)-mediated depletion of CHD8 on adipogenesis in the white preadipocyte cell line 3T3-L1 (Figure 1J). Adipogenesis and adipogenic gene expression were attenuated in these cells in a manner related to the extent of CHD8 depletion (Figures 1K and 1L), indicating that CHD8 is also important for adipocytic

(D) White preadipocytes derived from $Chd8_L^{F/F}$ mice and infected with retroviruses encoding Cre or EGFP were subjected to immunoblot analysis of CHD8 and HSP70 (loading control) as well as to qRT-PCR analysis of $Chd8_L$ mRNA. Quantitative data are means ± SD (n = 3 independent experiments). **p < 0.01 (Student's t test).

(E) $Chd8_L^{F/F}$ white preadipocytes infected with retroviruses encoding Cre or EGFP were induced to undergo adipogenesis for 8 days and then stained with oil red O.

(F) qRT-PCR analysis of adipogenic mRNAs in $Chd8_L^{F/F}$ white preadipocytes infected with retroviruses encoding Cre or EGFP and induced to undergo adipogenesis for 8 days. Data are means ± SD (n = 3 independent experiments). **p < 0.01 (Student's t test).

(G) Immunoblot and quantitative RT-PCR analyses of $Chd8_L$ expression in white preadipocytes derived from WT and $Chd8^{+/\Delta L}$ mice. Quantitative data are means ± SD (n = 4 independent experiments). **p < 0.01 (Student's t test).

(H) Oil red O staining of fat accumulation in WT and $Chd8^{+/\Delta L}$ white preadipocytes at 8 days after induction of adipogenesis.

(I) qRT-PCR analysis of adipogenic gene expression in WT and $Chd8^{+/\Delta L}$ white preadipocytes induced to undergo adipogenesis for 8 days. Data are means ± SD (n = 3 independent experiments). *p < 0.05, **p < 0.01 (Student's t test).

(J–L) 3T3-L1 cells infected with retroviruses encoding shRNAs specific for EGFP (control) or *Chd8* (*Chd8*-1 or *Chd8*-2) mRNAs were subjected to immunoblot analysis of CHD8 (J) or were induced to undergo adipogenesis for 8 days, after which fat accumulation was examined by staining with oil red O (K) and adipogenic gene expression was measured by qRT-PCR analysis (L). Quantitative data are means ± SD (n = 3 independent experiments). *p < 0.05, **p < 0.01 (Student's t test).

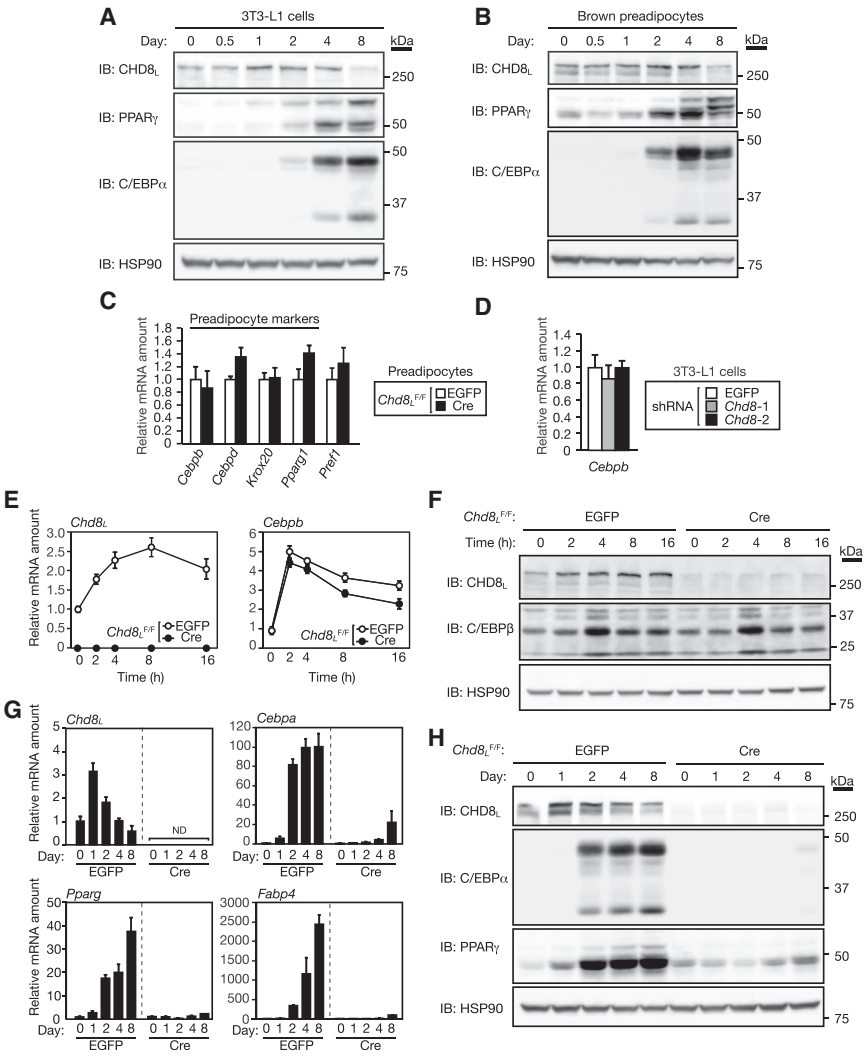

Figure 2. Deletion of *Chd8* Attenuates Induction of C/EBPα and PPARγ, but Not C/EBPβ

(A and B) Immunoblot analysis of CHD8 and preadipogenic marker proteins in 3T3-L1 cells (A) and brown preadipocytes (B) induced to undergo adipogenesis for 8 days.

(C) qRT-PCR analysis of preadipogenic mRNAs in $Chd8_L^{F/F}$ white preadipocytes infected with retroviruses encoding Cre or EGFP. Data are means ± SD (n = 3 independent experiments).

(D) qRT-PCR analysis of *Cebpb* mRNA in 3T3-L1 cells infected with retroviruses encoding shRNAs specific for EGFP (control) or *Chd8* mRNAs. Data are means ± SD (n = 3 independent experiments).

(E) qRT-PCR analysis of $Chd8_L$ and *Cebpb* mRNAs in $Chd8_L^{F/F}$ white preadipocytes infected with retroviruses encoding Cre or EGFP and treated with MDI for 16 hr. Data are means ± SD (n = 3 independent experiments).

(F) Immunoblot analysis of CHD8 and C/EBPβ in $Chd8_L^{F/F}$ white preadipocytes infected with retroviruses encoding Cre or EGFP and treated with MDI for 16 hr.

(G) qRT-PCR analysis of $Chd8_L$ and adipogenic mRNAs in $Chd8_L^{F/F}$ white preadipocytes infected with retroviruses encoding Cre or EGFP and induced to undergo adipogenesis for 8 days. Data are means ± SD (n = 3 independent experiments).

(H) Immunoblot analysis of CHD8, C/EBPα, and PPARγ in $Chd8_L^{F/F}$ white preadipocytes infected with retroviruses encoding Cre or EGFP and induced to undergo adipogenesis for 8 days.

differentiation of 3T3-L1 cells. Together, these results showed that CHD8 plays an essential role in adipogenesis *in vitro*.

CHD8 Directly Regulates *Cebpa* and *Pparg* Expression during Adipogenesis

To explore the mechanism underlying the impairment of adipogenesis in CHD8-deficient preadipocytes, we compared the expression of several adipogenic transcription factors between $Chd8_L^{-/-}$ and $Chd8_L^{F/F}$ preadipocytes during adipogenesis. We first showed that the expression of CHD8 was markedly upregulated as early as day 1 or 2 after the onset of adipogenic induction in 3T3-L1 cells or in brown preadipocytes isolated from WT mice (Figures 2A and 2B). Furthermore, ablation of CHD8 did not substantially affect the steady-state expression levels of preadipogenic genes such as *Cebpb*, *Cebpd*, *Krox20*, *Pparg1*, and *Pref1* in $Chd8_L^{F/F}$ preadipocytes or 3T3-L1 preadipocytes (Figures 2C and 2D). Whereas C/EBPβ, which functions upstream of *Cebpa* and *Pparg*, was induced normally at both mRNA and protein levels by MDI treatment in $Chd8_L^{-/-}$ preadipocytes (Figures 2E and 2F), the deletion of *Chd8* essentially prevented the activation of *Cebpa* and *Pparg* expression (Figures 2G and 2H).

We next investigated whether CHD8 might be associated with the promoter or enhancer regions of *Cebpa* or *Pparg* in preadipocytes of iWAT from WT mice using chromatin immunoprecipitation (ChIP) analysis (Guo et al., 2012; Wang et al., 2013). Endogenous CHD8 was indeed found to be associated with the promoter and enhancer regions of both *Cebpa* (Figure 3A) and *Pparg* (Figure 3B). No substantial association of CHD8 with the promoter region of *Runx2* (control) was detected (Figure 3A). CHD8 binding to *Cebpa* and *Pparg1* promoter regions was not affected by exposure of the cells to MDI, whereas that to the enhancer regions of both genes and to the *Pparg2* promoter region was upregulated (Figure 3C). Deletion of *Chd8* essentially abolished CHD8 association with the promoter and enhancer regions of *Cebpa* and *Pparg* (Figure 3D). Consistent with these results, forced expression of CHD8 increased *Cebpa* and *Pparg2* promoter activities in a concentration-dependent manner (Figure 3E). We also infected $Chd8_L^{-/-}$ preadipocytes with a retrovirus encoding PPARγ2. Such ectopic expression of PPARγ2 fully rescued adipogenesis in the CHD8-deficient preadipocytes (Figure 3F). Together, these results thus suggested that CHD8 interacts with the promoter and enhancer regions of *Cebpa* and *Pparg* and promotes transactivation of these genes during the early phase of adipogenesis.

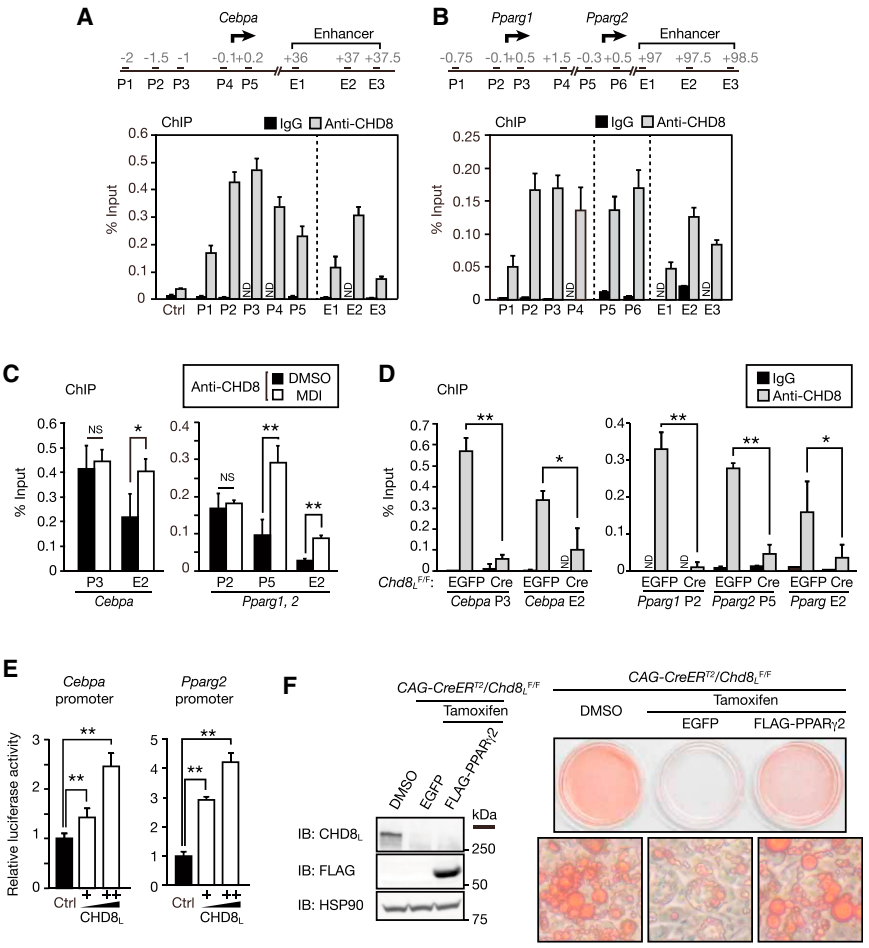

Figure 3. CHD8 Directly Regulates *Cebpa* and *Pparg* Expression in Preadipocytes

(A and B) ChIP analysis of CHD8 binding at *Cebpa* (A) and *Pparg* (B) loci in MDI-treated white preadipocytes. ChIP was performed with antibodies to CHD8 or control immunoglobulin G (IgG). Five promoter sites (P1–P5) and three enhancer sites (E1–E3) were tested for *Cebpa*, and six promoter sites (P1–P6), and three enhancer sites (E1–E3) were tested for *Pparg*. Site positions are indicated in kilobase pairs relative to the transcription start site (that of *Pparg2* for *Pparg* enhancer regions). The *Runx2* promoter region was also examined as a control (Ctrl) in (A). Data are means ± SD (n = 3 independent experiments). ND, not detected.

(C) Preadipocytes were exposed to MDI or DMSO (control) for 2 days and then subjected to ChIP with antibodies to CHD8. The precipitated DNA was quantitated by real-time PCR analysis with primers specific for *Cebpa* (P3 and E2) or *Pparg* (P3, P5, and E2). Data are means ± SD (n = 3 independent experiments). *p < 0.05, **p < 0.01 (Student's t test); NS, not significant.

(D) White $Chd8_L^{F/F}$ preadipocytes infected with retroviruses encoding Cre or EGFP were subjected to ChIP with antibodies to CHD8, and the precipitated DNA was quantitated by real-time PCR analysis with primers specific for *Cebpa* (P3 and E2) or for *Pparg* (P3, P5, and E2). Data are means ± SD (n = 3 independent experiments). *p < 0.05, **p < 0.01 (Student's t test).

(E) Luciferase reporter assays for HEK293T cells transfected with an expression vector for $CHD8_L$ (1 or 2 μg) and with a luciferase reporter plasmid containing the *Cebpa* or *Pparg2* promoter. Data are means ± SD (n = 3 independent experiments). **p < 0.01 (Student's t test).

(F) White *CAG-CreER*^{T2}/$Chd8_L^{F/F}$ preadipocytes (in which Cre recombinase is activated in response to tamoxifen exposure) were exposed to tamoxifen or DMSO vehicle for 2 days, infected with retroviruses encoding FLAG-epitope-tagged PPARγ2 or EGFP (control), and either subjected to immunoblot analysis with antibodies to CHD8 and to FLAG or induced to undergo adipogenesis for 8 days before staining with oil red O.

CHD8 Interacts with C/EBPβ and Regulates Adipogenic Gene Induction

Given that C/EBPβ is an upstream transcription factor of C/EBPα and PPARγ, we speculated that CHD8 might function cooperatively with C/EBPβ. Consistent with this notion, co-immunoprecipitation analysis revealed that FLAG-epitope-tagged C/EBPβ interacted with endogenous CHD8 in HEK293T cells and that endogenous C/EBPβ interacted with endogenous CHD8, but not with cyclin A (a nuclear protein examined as a negative control), in MDI-treated 3T3-L1 cells (Figures 4A–4C). Furthermore, luciferase reporter assays showed that CHD8 and C/EBPβ acted cooperatively to activate *Cebpa* and *Pparg2* promoters (Figure 4D). FAIRE (formaldehyde-assisted isolation of regulatory elements) analysis revealed a reduced extent of chromatin opening at the promoters of both *Cebpa* and *Pparg* in *Chd8*-deleted preadipocytes exposed to MDI compared with MDI-treated control cells (Figure 4E).

We next investigated whether the association of CHD8 with chromatin at *Cebpa* and *Pparg* loci is dependent on C/EBPβ. We depleted 3T3-L1 cells of C/EBPβ by shRNA-mediated RNAi and then examined whether the localization of CHD8 was affected. The amount of C/EBPβ protein in cells expressing the corresponding shRNA and exposed to MDI for 2 days was reduced to ~30% of that in control cells expressing an EGFP shRNA, whereas the abundance of CHD8 was not affected by C/EBPβ knockdown (Figure 4F). The binding of C/EBPβ to the *Pparg2* promoter was also correspondingly attenuated in the C/EBPβ-deficient cells (Figure 4G). ChIP analysis revealed that the extent of CHD8 binding to the *Cebpa* and *Pparg2* promoters in C/EBPβ-depleted cells was reduced compared with that in control cells (Figure 4H). In contrast, CHD8 binding to the *Pparg1* promoter, with which C/EBPβ does not interact (Siersbæk et al., 2011), was unaffected by the depletion of C/EBPβ (Figure 4H), suggesting that the attenuation of CHD8 binding to the *Cebpa* and *Pparg2* promoters was specific. These results thus indicate that the genomic localization of CHD8 is dependent, at least in part, on C/EBPβ. Conversely, the localization of C/EBPβ also appeared to be dependent on CHD8 (Figure 4I), suggesting that

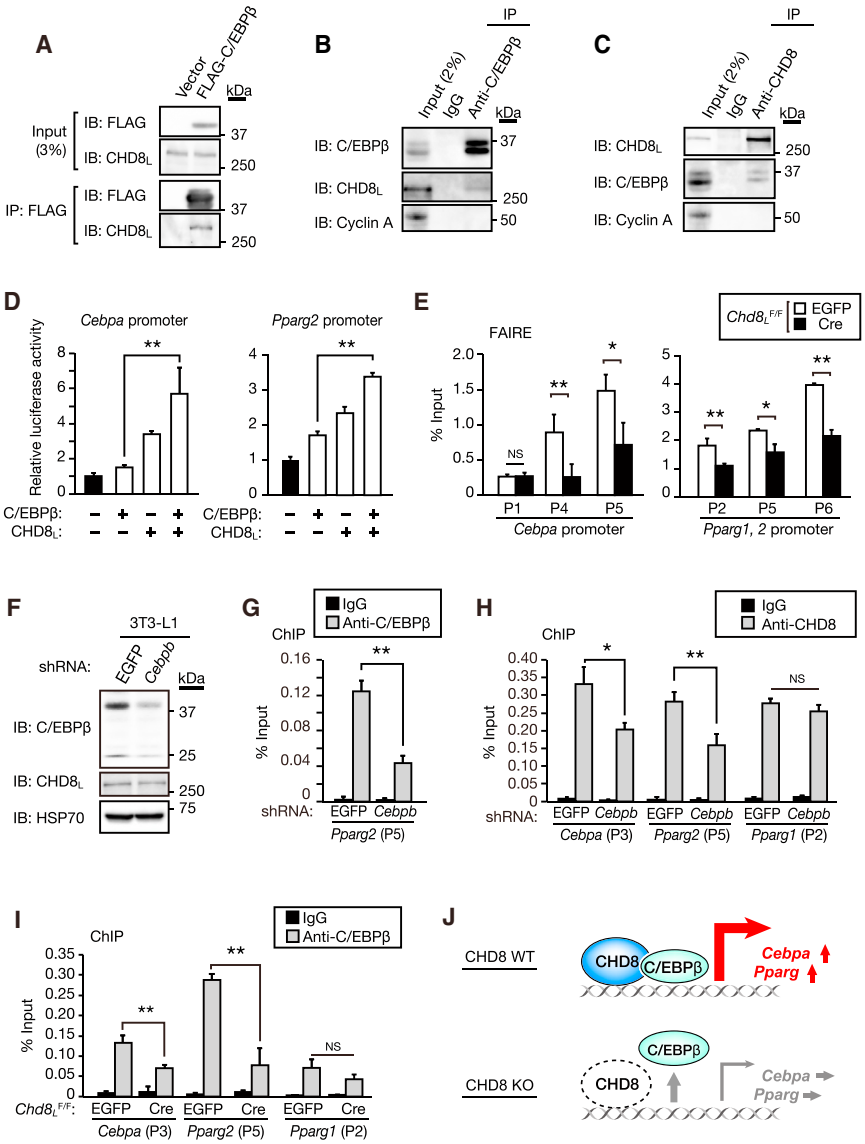

Figure 4. CHD8 Interacts with C/EBPβ and Upregulates Its Activity

(A) HEK293T cells expressing FLAG-tagged C/EBPβ were subjected to immunoprecipitation (IP) with antibodies to FLAG, and the resulting precipitates as well as the original cell lysates (3% of input) were subjected to immunoblot analysis with antibodies to FLAG and to CHD8. (B and C) White preadipocytes were induced to undergo adipogenesis for 1 day, after which nuclear extracts were prepared and subjected to immunoprecipitation with antibodies to C/EBPβ (B) or CHD8 (C). The resulting precipitates were subjected to immunoblot analysis with the same antibodies. Cyclin A was examined as a loading control.

(D) Luciferase reporter assays for HEK293T cells transfected with expression vectors for $CHD8_L$ or C/EBPβ as well as with luciferase reporter plasmids containing the *Cebpa* or *Pparg2* promoters. Data are means ± SD (n = 3 independent experiments). **p < 0.01 (Student's t test).

(E) White $Chd8_L^{F/F}$ preadipocytes infected with retroviruses encoding Cre or EGFP were induced to undergo adipogenesis for 2 days and were then subjected to FAIRE analysis of chromatin opening at promoter regions of *Cebpa* and *Pparg*. Data are means ± SD (n = 3 independent experiments). *p < 0.05, **p < 0.01 (Student's t test).

(F–H) 3T3-L1 cells infected with retroviruses encoding shRNAs specific for EGFP or *Cebpb* mRNAs were induced to undergo adipogenesis for 2 days and then subjected either to immunoblot analysis of C/EBPβ and CHD8 (F) or to ChIP analysis of *Cebpa* or *Pparg* promoters with antibodies to C/EBPβ (G) or CHD8 (H). Quantitative data are means ± SD (n = 3 independent experiments). *p < 0.05, **p < 0.01 (Student's t test).

(I) $Chd8_L^{F/F}$ preadipocytes infected with retroviruses encoding Cre or EGFP were subjected to ChIP analysis of *Cebpa* and *Pparg* promoters with antibodies to C/EBPβ at 2 days after MDI treatment. Data are means ± SD (n = 3 independent experiments). **p < 0.01 (Student's t test).

(J) Model for CHD8 function during adipogenesis. CHD8 interacts with C/EBPβ and upregulates the expression of *Cebpa* and *Pparg* by remodeling their promoters to an open chromatin state that is necessary for adipogenesis. Loss of CHD8 (KO) reduces chromatin accessibility and C/EBPβ binding to the promoter regions.

CHD8 and C/EBPβ bind to genomic sites in a mutually dependent manner (Figure 4J).

CHD8 Colocalizes with C/EBPβ at the Genome-wide Level

To determine the extent of colocalization of CHD8 and C/EBPβ at the genome-wide level, we performed ChIP and sequencing (ChIP-seq) analysis with antibodies to CHD8 in 3T3-L1 cells at 4 hr after the onset of MDI treatment. The resulting data were then integrated with published ChIP-seq and DNaseI-hypersensitive site (DHS)-sequencing profiles (Siersbæk et al., 2011). A total of 71,830 CHD8 peaks were detected, and these peaks were annotated on the basis of genomic features. Most of the peaks localized to intergenic (34%), intron (26%), and transcription start site (TSS; 25%) regions (Figure 5A). Approximately half of genes (53%) had one or more CHD8 peaks within ±50 kbp from the TSS (Figure 5B). We found that 16% of CHD8 peaks overlapped with DHSs, and that 20% of these peaks colocalized with C/EBPβ peaks, including those associated with typical C/EBPβ target genes such as *Cebpa*, *Klf5*, *Pparg2*, and *Wnt10b* (Figures 5C–5E). The vast majority of CHD8 peaks that overlapped with C/EBPδ, the glucocorticoid receptor (GR), signal transducer and activator of transcription 5A (STAT5A), or the retinoid X receptor (RXR) were also occupied by C/EBPβ (Figure 5F), although the colocalization rate of CHD8 with these four transcription factors was low (Figure 5D). These results

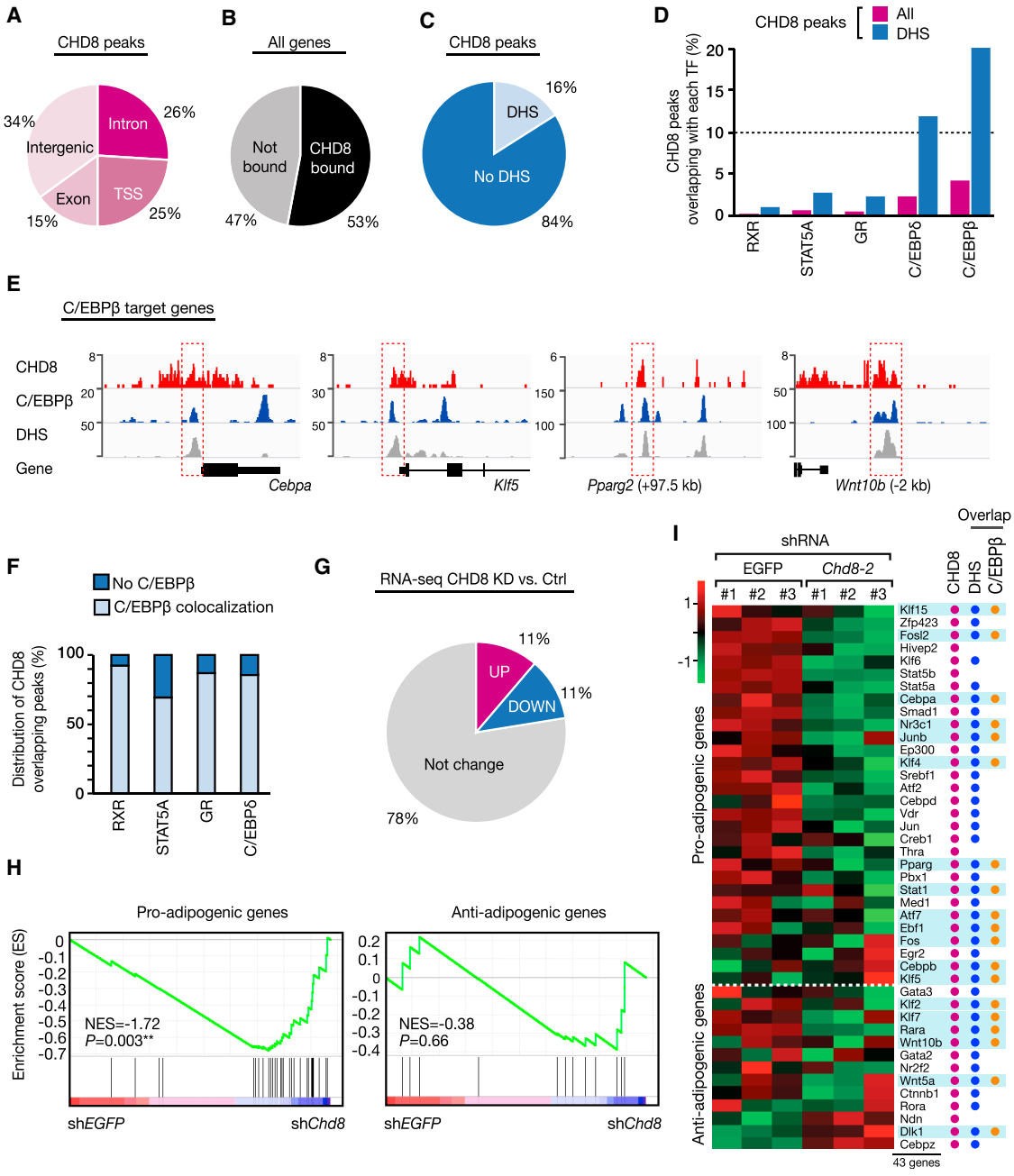

Figure 5. CHD8 Colocalizes with C/EBPβ at Genomic Sites and Regulates Adipogenic Genes

(A) Distribution of CHD8 binding peaks among features of the mouse genome as determined by ChIP-seq analysis of 3T3-L1 cells at 4 hr after the onset of exposure to MDI. "TSS" denotes the region spanning −2 to +2 kbp relative to the actual TSS.

(B) Classification of all genes according to whether they are direct targets of CHD8 as determined by ChIP-seq. Direct targets of CHD8 were defined by the presence of one or more CHD8 peaks within ±50 kbp from the TSS.

(C) CHD8 binding peaks classified according to whether they overlap with DHS peaks.

(D) All CHD8 binding peaks or those that overlap with DHSs were subdivided on the basis of whether they overlap with binding peaks for the transcription factors (TFs) RXR, STAT5A, GR, C/EBPδ, or C/EBPβ.

(E) CHD8 ChIP-seq, C/EBPβ ChIP-seq, and DHS-seq data for representative target genes of C/EBPβ viewed in the IGV genome browser. Boxed regions indicate overlapping peaks.

(F) Classification of CHD8 peaks that overlap with those of the indicated transcription factors according to whether or not they also overlap with C/EBPβ peaks.

(legend continued on next page)

thus indicated that CHD8 mainly colocalizes with C/EBPβ at open chromatin sites and that the two proteins regulate the expression of adipogenic genes in a cooperative manner.

We next performed RNA sequencing (RNA-seq) analysis in CHD8-depleted and control 3T3-L1 cells at 12 h after the onset of MDI treatment and then integrated the resulting data with those of our ChIP-seq analysis with antibodies to CHD8. RNA-seq analysis revealed that the expression of 11% of genes was upregulated and that of 11% of genes was downregulated in the CHD8-depleted cells (Figure 5G; Data S1). We also examined our ChIP-seq and RNA-seq data for 43 key adipogenesis-associated genes highlighted in recent reviews (Siersbæk et al., 2012; Stephens, 2012). Gene set enrichment analysis (GSEA) revealed a significant decrease in the expression of pro-adipogenic genes in the cells depleted of CHD8 compared with control cells, whereas anti-adipogenic genes did not show enrichment (Figure 5H). ChIP-seq analysis revealed that all 43 adipogenic genes had CHD8 peaks, with these peaks in 39 of the genes overlapping with DHSs, whereas 47% of all genes did not have CHD8 peaks (Figures 5B and 5I). We identified 19 genes at which CHD8 and C/EBPβ colocalized, including *Cebpa* and *Pparg*, suggesting that the two proteins cooperate to promote the expression of these adipogenic genes. Collectively, our results thus suggested that CHD8 regulates the expression of many adipogenic genes in association with C/EBPβ and thereby promotes adipogenesis.

CHD8 Is Essential for WAT Development

To investigate CHD8 function *in vivo*, we generated *Prx1-Cre/Chd8*$_L^{F/F}$ mice by crossing *Chd8*$_L^{F/F}$ mice with *Prx1-Cre* mice. Expression of *Prx1-Cre* in adipose tissue is limited to preadipocytes of iWAT, rendering *Prx1-Cre*-dependent recombination useful for depot-restricted genetic manipulation (Figure 6A) (Krueger et al., 2014; Sanchez-Gurmaches et al., 2015). To examine whether *Prx1-Cre*-dependent deletion of *Chd8* inhibits adipogenesis, we fed *Prx1-Cre/Chd8*$_L^{F/F}$ mice and *Chd8*$_L^{F/F}$ (control) mice either a low-fat diet (LFD) or a high-fat diet (HFD) for 11 weeks beginning at 4 weeks of age. Although body weight was similar in *Prx1-Cre/Chd8*$_L^{F/F}$ mice and *Chd8*$_L^{F/F}$ mice fed either diet (Figure 6B), the gross appearance of iWAT was substantially affected in the former animals (Figures 6C, 6D, and S1A). Computed tomography (CT) also revealed that subcutaneous fat mass was markedly reduced in *Prx1-Cre/Chd8*$_L^{F/F}$ mice fed either diet compared with control mice, whereas visceral fat mass did not differ between the two genotypes (Figures 6E and 6F). Although gonadal WAT (gWAT) weight and interscapular BAT weight were similar in *Prx1-Cre/Chd8*$_L^{F/F}$ mice and *Chd8*$_L^{F/F}$ mice (Figures 6G, 6H, and S1B), iWAT weight was significantly smaller in the former animals fed either an LFD or HFD (Figure 6I).

CHD8 Controls Adipogenesis and Adipocyte Hypertrophy *in Vivo*

Histological analysis showed that the area of vascular tissue in iWAT was increased in *Prx1-Cre/Chd8*$_L^{F/F}$ mice fed an LFD compared with control animals, whereas adipocyte size did not differ between the two genotypes (Figure 6J). In contrast, the size of adipocytes in iWAT of *Prx1-Cre/Chd8*$_L^{F/F}$ mice fed an HFD was reduced compared with that in control mice (Figures 6K and 6L). The amounts of mRNAs for preadipogenic genes were increased, whereas those of mRNAs for adipogenic genes were greatly reduced, in iWAT of *Prx1-Cre/Chd8*$_L^{F/F}$ mice fed an LFD compared with control mice (Figure 6M), suggesting that the smaller fat mass of *Prx1-Cre/Chd8*$_L^{F/F}$ mice maintained on such a diet was attributable to reduced adipogenesis. The expression levels of adipogenic genes in iWAT of *Prx1-Cre/Chd8*$_L^{F/F}$ mice fed an HFD were also reduced compared with those in control mice, suggesting that the smaller fat mass of the mutant animals fed an HFD is attributable to reduced adipogenesis and adipocyte hypertrophy (Figure 6N). Consistent with these observations, preadipocytes isolated from *Prx1-Cre/Chd8*$_L^{F/F}$ mice were impaired in the ability to form mature adipocytes (Figures S1C–S1E).

To examine whether CHD8 is essential for HFD-induced adipocyte hypertrophy, we generated *CAG-CreER*^{T2}*/Chd8*$_L^{F/F}$ mice by crossing *Chd8*$_L^{F/F}$ mice with *CAG-CreER*^{T2} mice. We then administered tamoxifen to 6-week-old *CAG-CreER*^{T2}*/Chd8*$_L^{F/F}$ mice by oral gavage for five consecutive days and confirmed that almost all floxed alleles were inactivated in preadipocytes derived from iWAT of the treated animals (Figure 7A). Tamoxifen-treated *CAG-CreER*^{T2}*/Chd8*$_L^{F/F}$ mice fed an HFD beginning after the end of tamoxifen administration showed a significantly reduced body weight, fat mass, and WAT weight compared with *Chd8*$_L^{F/F}$ (control) mice (Figures 7B–7F). Moreover, the size of adipocytes (Figure 7G) as well as the expression levels of adipogenic genes (Figure 7H) in iWAT of tamoxifen-treated *CAG-CreER*^{T2}*/Chd8*$_L^{F/F}$ mice fed an HFD were reduced compared with those in control mice. Collectively, these results suggested that CHD8 is required in a cell-autonomous manner for both adipogenesis and adipocyte hypertrophy during WAT development.

DISCUSSION

We have shown that CHD8 interacts with C/EBPβ and positively regulates C/EBPα and PPARγ gene expression during adipogenesis. Deletion of *Chd8* specifically in preadipocytes of iWAT resulted in a marked reduction in corresponding adipose tissue mass, suggesting that impairment of adipogenesis occurs in a cell-autonomous manner. Although individuals with ASD in general tend to be overweight or prone to obesity (Curtin et al., 2010, 2014; Zheng et al., 2017), those with *CHD8* mutations tend to be slender (Bernier et al., 2014). We now conclude that this latter phenotype is not the result of a neurodevelopmental defect but is instead due to impairment of adipogenesis.

Adipogenesis is controlled by a complex network of transcription factors that mediate the differentiation of preadipocytes into mature adipocytes (Rosen and MacDougald, 2006). In the early

(G) Distribution of genes whose expression was upregulated or downregulated in CHD8-depleted (KD) 3T3-L1 cells at 12 hr after the onset of exposure to MDI compared with control (Ctrl) cells as determined by RNA-seq analysis. Differentially expressed genes were defined as $\log_2$ fold change > 0.3 or < −0.3.
(H and I) Effect of CHD8 knockdown on the expression of key genes related to adipogenesis as determined by the RNA-seq analysis of 3T3-L1 cells. Gene expression changes are shown as GSEA plots (H) and a heatmap (I). Overlap of CHD8 binding peaks with DHS and C/EBPβ peaks is indicated for each gene.

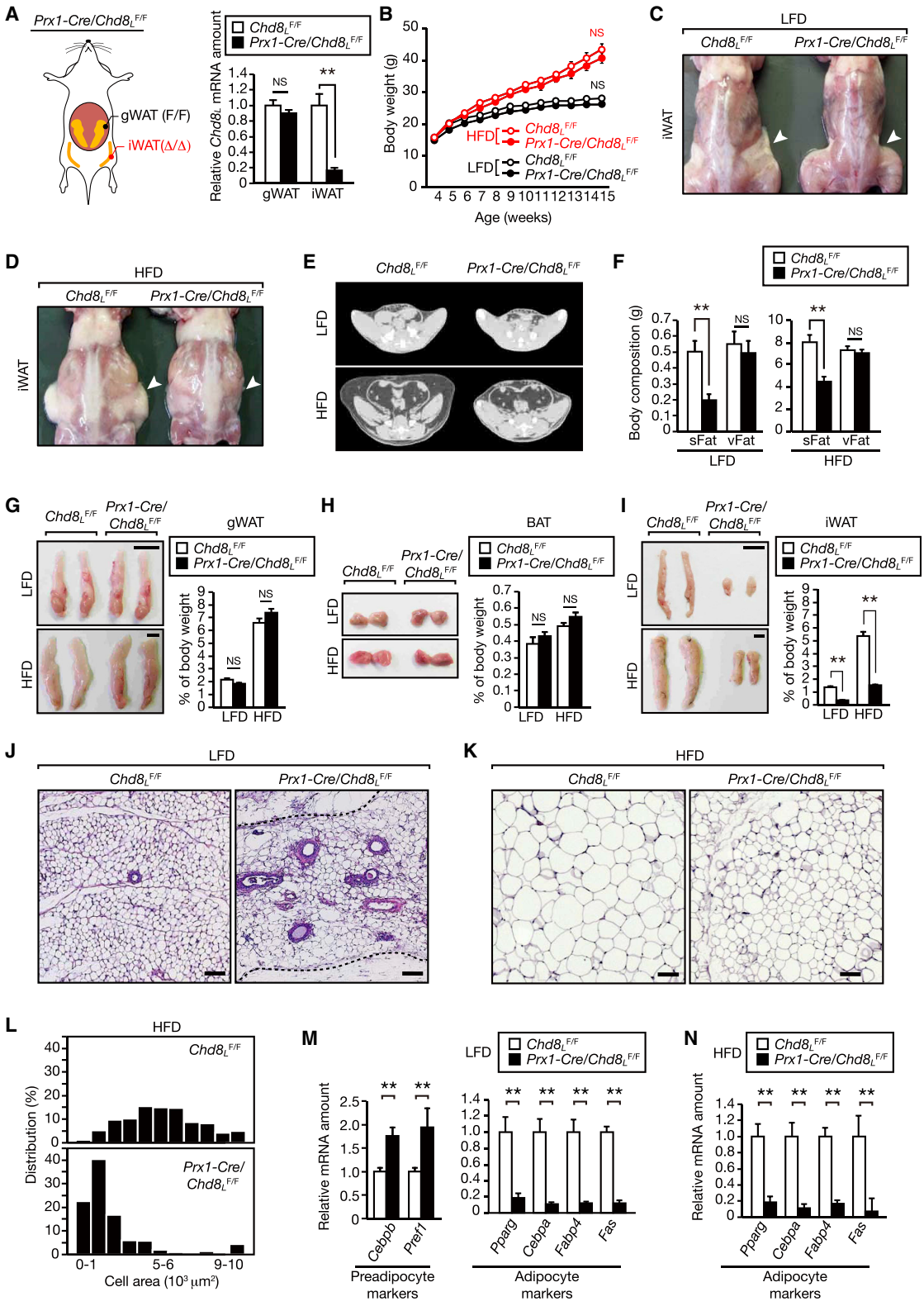

Figure 6. Attenuated Adipogenesis and Adipocyte Hypertrophy in iWAT of *Prx1-Cre/Chd8*$_L^{F/F}$ Mice

(A) Schematic representation of the limitation of *Prx1-Cre* expression to preadipocytes of iWAT, and qRT-PCR analysis of *Chd8*$_L$ mRNA in iWAT and gWAT of *Prx1-Cre/Chd8*$_L^{F/F}$ and *Chd8*$_L^{F/F}$ mice at 4 weeks of age. Data are means ± SEM (n = 5). **p < 0.01 (Student's t test).

(legend continued on next page)

phase of adipogenesis, multiple adipogenic signals activate a variety of preadipogenic transcription factors, including C/EBPβ, C/EBPδ, GR, and STAT5A, that colocalize at transcriptional regulatory regions of the genome and coordinate the assembly of functional "hotspots," resulting in transcriptional activation of target genes such as *Cebpa* and *Pparg* via DNA looping and interaction with promoter regions (Siersbæk et al., 2014). Our results now identify CHD8 as an important coactivator of C/EBPβ in this process, with the extent of CHD8 association with transcriptional regulatory regions of *Cebpa* and *Pparg* increasing in response to adipogenic stimulation. Our results thus suggest that adipogenic stimulation induces binding of CHD8 to transcription regulatory regions or to preadipogenic transcription factors, including C/EBPβ, and that such association is required for proper adipogenesis. Given that dynamic chromatin loops that link promoter and enhancer regions are implicated in regulation of the expression of specific genes during adipogenesis (Siersbaek et al., 2017), we speculate that CHD8 might play a role in mediating such interactions. The molecular mechanism underlying these promoter-enhancer interactions and the identity of transcription factors that may function with CHD8 remain to be elucidated.

An increase in both adipocyte cell size (hypertrophy) and number (hyperplasia) is required for adipose tissue growth. We have shown that both the formation of adipocytes (adipogenesis) and subsequent adipocyte hypertrophy were abrogated in WAT of CHD8-deficient mice (Figure 6), whereas cells in which *Chd8* was deleted by retroviral expression of Cre recombinase *in vitro* showed only a defect in adipogenesis (Figure 1E). One possible explanation for these findings is that although CHD8 is indispensable for both adipogenesis and adipocyte hypertrophy, $Chd8_L$ deletion due to Cre expression driven by the *Prx1* promoter *in vivo* is not complete during adipogenesis, with the result that some cells undergo delayed *Chd8* deletion after adipogenesis and then manifest a defect in adipocyte hypertrophy. In contrast, the efficiency of $Chd8_L$ deletion due to retrovirus-mediated Cre expression in $Chd8_L^{F/F}$ preadipocytes *in vitro* appears to be ~100%, with the resulting almost complete block of adipogenesis precluding manifestation of the effect of CHD8 loss on adipocyte hypertrophy (Figure S2).

Adipocytes play a central role in energy storage, lipid metabolism, and glucose homeostasis (Rosen and Spiegelman, 2006). Given that excessive adipocyte hypertrophy and hyperplasia lead to obesity and obesity-related disorders such as type 2 diabetes, hypertension, hyperlipidemia, and arteriosclerosis, a full understanding of adipogenesis is important for elucidation of the mechanisms underlying these various conditions (Muir et al., 2016). Our identification of the role of CHD8 in this process provides a basis for the development of potential treatments for obesity and type 2 diabetes.

EXPERIMENTAL PROCEDURES

Mice

Generation of $Chd8_L^{+/-}$ and $Chd8_L^{F/F}$ mice was described previously (Katayama et al., 2016). $Chd8_L^{F/F}$ mice were crossed with *Prx1-Cre* transgenic mice to generate *Prx1*-Cre/$Chd8_L^{F/F}$ mice and with *CAG-CreER*^{T2} mice to generate *CAG-CreER*^{T2}/$Chd8_L^{F/F}$ mice. All manipulated mice were backcrossed with C57BL/6 mice for >10 generations. Mice were fed either an LFD (D12450B, Research Diets) or an HFD (D12492, Research Diets). CT scans for measurement of fat and lean body mass were performed with a Latheta LTC-100 instrument (Aloka). All animals were maintained under the specific-pathogen-free condition, and all experiments were approved by the animal ethics committee of Kyushu University. Data are shown for male mice.

Cell Culture

Preadipocytes were isolated from iWAT of mice at 4 weeks of age or from interscapular BAT of mice at 2 days of age by digestion with Liberase TM (50 μg/mL, Sigma) and were immortalized by transfection with a plasmid containing SV40 genomic DNA (kindly provided by T. Akagi, KAN Research Institute, Kobe, Japan). Preadipocytes, 3T3-L1 cells, Plat-E cells, and HEK293T cells were maintained in DMEM supplemented with 10% fetal bovine serum (Invitrogen), 1 mM sodium pyruvate, penicillin (100 U/mL), streptomycin (100 mg/mL), 2 mM L-glutamine, nonessential amino acids (10 ml/L) (Invitrogen), and, in the case of Plat-E cells, blasticidin (10 μg/mL).

Adipogenesis Assay

Cells were plated at a density of 5×10^5 per 35-mm dish, and differentiation toward the adipocyte lineage was induced by exposure for 2 days to insulin (5 μg/mL), 0.5 mM 3-isobutyl-1-methyl-xanthine, and 1 μM dexamethasone. The cells were then maintained in medium containing insulin (5 μg/mL) alone, which was replenished every other day. For detection of fat accumulation, cells were washed twice with PBS, fixed in 3.7% formaldehyde for 10 min, and stained for 20 min with 0.18% oil red O in 60% isopropanol.

Retrovirus Expression System

A complementary DNA encoding mouse PPARγ2 with an NH_2-terminal FLAG tag was subcloned into pMX-puro (kindly provided by T. Kitamura, University of Tokyo, Japan) with the Gateway vector conversion system. The resulting vectors were introduced into Plat-E packaging cells by transfection in order

(B) Time course of body weight for $Chd8_L^{F/F}$ and *Prx1-Cre*/$Chd8_L^{F/F}$ mice fed an LFD or HFD. Data are means ± SEM (n = 6 to 8). NS, not significant by Student's t test.
(C and D) Gross appearance of 15-week-old $Chd8_L^{F/F}$ and *Prx1-Cre*/$Chd8_L^{F/F}$ mice fed an LFD (C) or HFD (D). Arrowheads indicate iWAT.
(E and F) CT images of the abdomen (E) and quantitation of subcutaneous (s) and visceral (v) fat (F) for $Chd8_L^{F/F}$ and *Prx1-Cre*/$Chd8_L^{F/F}$ mice at 15 weeks of age. Quantitative data are means ± SEM (n = 8). **p < 0.01 (Student's t test).
(G–I) Gross appearance and weight of gWAT (G), interscapular BAT (H), and iWAT (I) in $Chd8_L^{F/F}$ and *Prx1-Cre*/$Chd8_L^{F/F}$ mice at 15 weeks of age. Quantitative data are means ± SEM (n = 6–8). Scale bars, 10 mm. **p < 0.01 (Student's t test).
(J and K) H&E staining of iWAT sections for LFD-fed (J) or HFD-fed (K) $Chd8_L^{F/F}$ and *Prx1-Cre*/$Chd8_L^{F/F}$ mice at 15 weeks of age. Dashed lines indicate boundary of iWAT. Scale bars, 100 μm.
(L) Adipocyte size distribution for iWAT of HFD-fed $Chd8_L^{F/F}$ and *Prx1-Cre*/$Chd8_L^{F/F}$ mice at 15 weeks of age. Data are means (n = 3).
(M) qRT-PCR analysis of adipogenic gene expression in iWAT of LFD-fed $Chd8_L^{F/F}$ and *Prx1-Cre*/$Chd8_L^{F/F}$ mice at 15 weeks of age. Data are means ± SEM (n = 5). **p < 0.01 (Student's t test).
(N) qRT-PCR analysis of adipogenic gene expression in iWAT of HFD-fed $Chd8_L^{F/F}$ and *Prx1-Cre*/$Chd8_L^{F/F}$ mice at 15 weeks of age. Data are means ± SEM (n = 5). **p < 0.01 (Student's t test).
See also Figure S1.

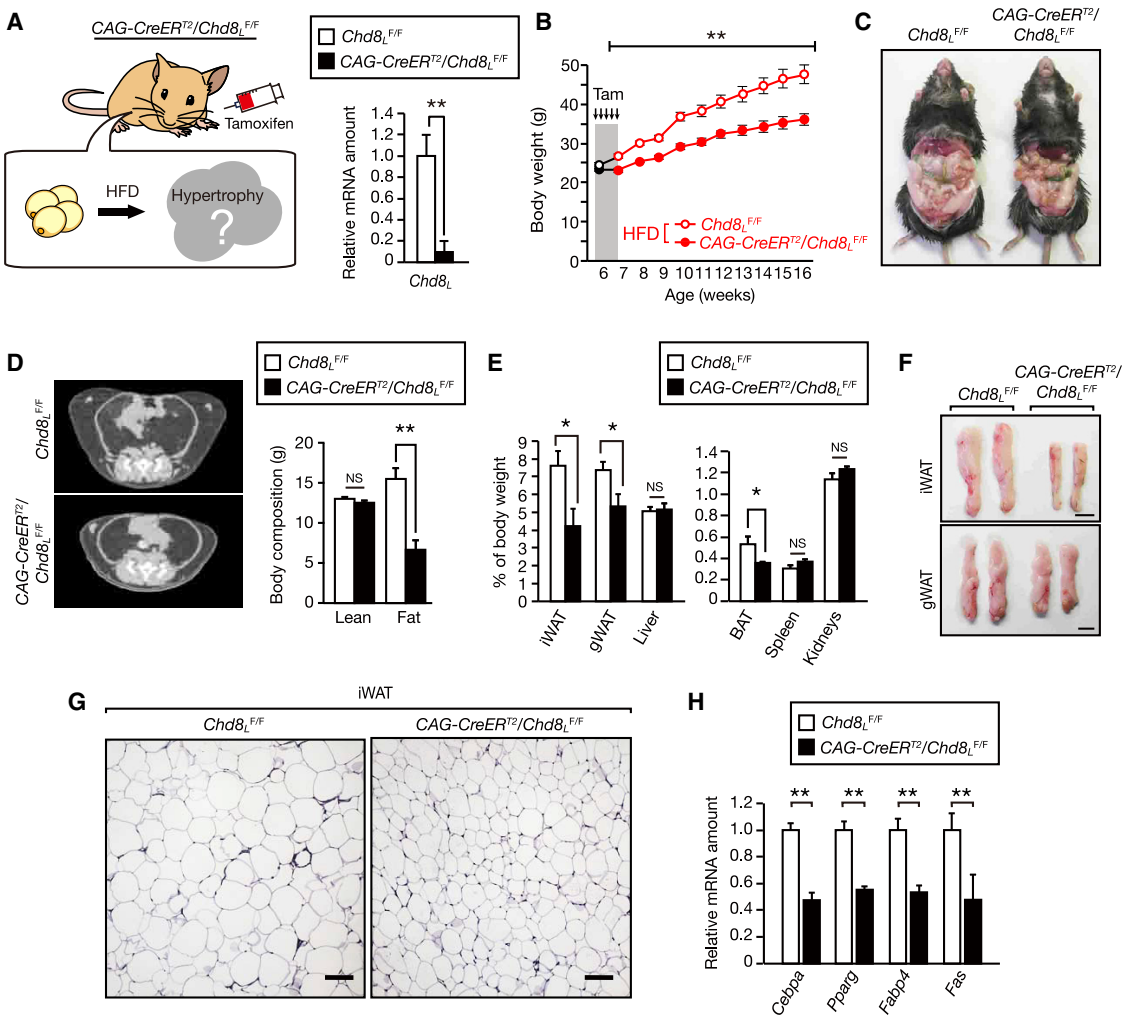

Figure 7. Inducible Knockout of *Chd8* in Adult Mice Protects against Adipocyte Hypertrophy

(A) Schematic representation of the experimental protocol as well as qRT-PCR analysis of $Chd8_L$ mRNA in the preadipocyte fraction of iWAT from 7-week-old *CAG-CreER*^{T2}/$Chd8_L^{F/F}$ or $Chd8_L^{F/F}$ mice that had been treated with tamoxifen for five consecutive days at 6 weeks of age. Data are means ± SEM (n = 4). **p < 0.01 (Student's t test).

(B) Time course of body weight for tamoxifen (Tam)-treated $Chd8_L^{F/F}$ and *CAG-CreER*^{T2}/$Chd8_L^{F/F}$ mice fed an HFD. Data are means ± SEM (n = 8). **p < 0.01 (Student's t test).

(C) Gross appearance of tamoxifen-treated $Chd8_L^{F/F}$ and *CAG-CreER*^{T2}/$Chd8_L^{F/F}$ mice fed an HFD up to 20 weeks of age.

(D) CT images of the abdomen and measurement of fat and lean mass for mice as in (C). Quantitative data are means ± SEM (n = 8). **p < 0.01 (Student's t test).

(E and F) Mass (E) and gross appearance (F) of iWAT, gWAT, interscapular BAT, liver, spleen, or kidneys for mice as in (C). Scale bars, 10 mm. Quantitative data are means ± SEM (n = 8). *p < 0.05 (Student's t test).

(G) H&E staining of iWAT sections from mice as in (C). Scale bars, 100 μm.

(H) qRT-PCR analysis of adipogenic gene expression in the adipocyte fraction of iWAT of mice as in (C). Data are means ± SEM (n = 8). **p < 0.01 (Student's t test).

to generate recombinant retroviruses. Preadipocytes were infected with retroviruses in the presence of polybrene (5 μg/ml) and were then cultured in the presence of puromycin (5 μg/mL).

RNA Interference

A retroviral vector for expression of shRNAs was described previously (Kita et al., 2012).

The hairpin sequences specific for mouse *Chd8* mRNA (*Chd8*-1 and *Chd8*-2), *Cebpb* mRNA, or EGFP mRNA (control) corresponded to nucleotides 138–158 (*Chd8*-1), 814–834 (*Chd8*-2), 657–677 (*Cebpb*), and 126–146 (EGFP) of the respective coding regions. The shRNA vectors were introduced into Plat-E cells for generation of recombinant retroviruses. 3T3-L1 cells were infected with retroviruses in the presence of polybrene (5 μg/mL) and were then cultured in the presence of puromycin (5 μg/mL).

Luciferase Assay

Fragments (2,000 bp) of mouse genomic DNA containing the TSS of *Cebpa* or *Pparg2* were subcloned into the pGL3-Basic vector (Promega). A 1,200-bp fragment of mouse genomic DNA containing the TSS of *Rosa26* was subcloned into the pRL null vector (Promega). HEK293T cells were seeded at a density of 3 × 10^5 per well in six-well plates 24 hr before transfection with target promoter constructs (0.4 μg), the control vector pRL-*Rosa26* (0.1 μg), and the expression vector for $CHD8_L$ (1 or 2 μg) using the FuGENE HD reagent (Promega). Luciferase activity was measured with a Dual-Luciferase Reporter

Assay System (Promega) and a Lumat^3 LB9508 luminometer at 24 hr after transfection. Firefly luciferase activity was normalized by that of *Renilla* luciferase.

RT-PCR and Real-Time PCR Analysis

Total RNA (1 μg) isolated from cells or tissue using Isogen (Nippon Gene) was subjected to RT-PCR with ReverTra Ace-α (Toyobo), and the resulting cDNA was subjected to real-time PCR analysis with SYBR Premix EX Taq (TaKaRa) and specific primers in a Step One Plus Real-Time PCR System (Applied Biosystems). Data were normalized by the abundance of *Arbp* mRNA. Primer sequences are provided in Table S1.

Transfection

Complementary DNAs encoding mouse C/EBPβ or CHD8$_L$, each tagged at its NH_2-terminus with the FLAG epitope, were subcloned into pcDNA3 (Invitrogen). HEK293T cells were transfected with expression vectors with the use of the FuGENE HD reagent (Promega).

Immunoblot Analysis

Total protein extracts were prepared from preadipocytes, adipocytes, and WAT with a lysis buffer containing 50 mM Tris-HCl (pH 7.5), 150 mM NaCl, 0.5% Triton X-100, 10 mM NaF, 10 mM $Na_4P_2O_7$, 0.4 mM Na_3VO_4, 0.4 mM EDTA, leupeptin (20 μg/mL), aprotinin (10 μg/mL), and 1 mM phenylmethylsulfonyl fluoride. The extracts (30 μg protein) were subjected to immunoblot analysis as previously described (Kita et al., 2012).

Immunoprecipitation

Nuclear extracts of MDI-treated preadipocytes were incubated for 1 hr at 4°C with the indicated antibodies immobilized on Dynabeads (Thermo Fisher Scientific). The beads were then washed three times with lysis buffer, and the immunoprecipitated proteins were subjected to immunoblot analysis.

Antibodies

Antibodies to PPARγ (sc-7273), C/EBPβ (sc-150), and cyclin A (sc-751) were obtained from Santa Cruz Biotechnology; those to C/EBPα (D56F10) were from Cell Signaling, those to HSP70 (610608) and HSP90 (610419) were from Transduction Laboratories, and those to FLAG (M2) were from Sigma. Horseradish-peroxidase-conjugated antibodies to rabbit immunoglobulin G (TrueBlot, 18-8816-31) were obtained from Rockland. Polyclonal antibodies to CHD8 for immunoblot analysis were generated by A. Kikuchi (Hiroshima University, Japan), and monoclonal antibodies to CHD8 for ChIP analysis were generated by Y. Katayama.

ChIP and FAIRE

ChIP assays were performed as previously described with 2×10^6 cells for each reaction (Katayama et al., 2016). FAIRE assays were also performed as previously described with 1×10^6 cells for each reaction (Simon et al., 2012). All primer sequences are listed in Table S2.

ChIP-Seq

ChIP-seq was performed essentially as described previously (Odawara et al., 2011). 3T3-L1 cells in a 10-cm dish at 4 hr after the onset of adipogenic stimulation were subjected to ChIP with antibodies to CHD8 as described above, and the precipitated and purified DNA was sequenced with a HiSeq 1500 system (Illumina). Reads were uniquely mapped to the mouse (mm9) genome using Bowtie software (version 1.2.2), and duplicated reads were removed with Picard (version 2.17.6). Markedly enriched regions of the genome were identified with the MACS peak caller (version 2.1.1, with the option "–gsize mm–nomodel–to-large"). ChIP-seq analysis was performed with biological duplicates.

RNA-Seq

Total RNA was extracted from 3T3-L1 cells 12 hr after the onset of adipogenic stimulation with the TRIzol Plus RNA Purification Kit (Life Technologies). RNA-seq was performed as described previously (Odawara et al., 2011). Complementary DNA was sequenced with a HiSeq 1500 system (Illumina). The total amount of each transcript was calculated using a series of programs, including TopHat (version 2.1.1) and Cufflinks (version 2.2.1). RNA-seq reads were mapped to the mouse (mm9) genome. Normalized expression data were analyzed with GSEA v2.0.13 software (Broad Institute, Cambridge, MA).

Histopathology

Tissue was fixed with 4% formaldehyde in PBS, embedded in paraffin, sectioned with a cryostat at a thickness of 5 μm, and stained with H&E.

Statistical Analysis

Quantitative data are presented as means ± SEM or means ± SD as indicated and were compared between groups with the two-tailed Student's t test as performed with Microsoft Excel software. A p value of < 0.05 was considered statistically significant.

DATA AND SOFTWARE AVAILABILITY

The accession number for the sequencing data reported in this paper is DRA: DRA006663.

SUPPLEMENTAL INFORMATION

Supplemental Information includes two figures, two tables, and one dataset and can be found with this article online at https://doi.org/10.1016/j.celrep.2018.04.050.

ACKNOWLEDGMENTS

We thank T. Kitamura and T. Akagi for providing vectors and DNA; N. Nishimura, K. Tsunematsu, and other laboratory members for technical assistance; and A. Ohta for help in preparation of the manuscript. This study was funded in part by KAKENHI grants (2522130, 26640080, and 17H06301) from the Ministry of Education, Culture, Sports, Science, and Technology (MEXT) of Japan. It was also supported in part by a Japan Society for the Promotion of Science (JSPS) fellowship (13J04520) to Y. Kita.

AUTHOR CONTRIBUTIONS

Y. Kita planned and performed all experiments. Y. Katayama created *Chd8*$^{+/\Delta L}$ and *Chd8*$_L^{F/F}$ mice, performed experiments, and provided intellectual support. T. Shiraishi, K.M., and T.O. assisted with experiments. Y. Ohkawa, M. Suyama and T. Sato performed sequencing and data analysis. M.N. and M. Shirane provided materials and intellectual support. Y. Oike provided intellectual support. K.I.N. coordinated the study, oversaw the results and wrote the manuscript. All authors discussed the results and commented on the manuscript.

DECLARATION OF INTERESTS

The authors declare no competing interests.

Received: June 10, 2017
Revised: March 28, 2018
Accepted: April 12, 2018
Published: May 15, 2018

REFERENCES

Bagchi, A., Papazoglu, C., Wu, Y., Capurso, D., Brodt, M., Francis, D., Bredel, M., Vogel, H., and Mills, A.A. (2007). CHD5 is a tumor suppressor at human 1p36. Cell *128*, 459–475.

Bajpai, R., Chen, D.A., Rada-Iglesias, A., Zhang, J., Xiong, Y., Helms, J., Chang, C.P., Zhao, Y., Swigut, T., and Wysocka, J. (2010). CHD7 cooperates with PBAF to control multipotent neural crest formation. Nature *463*, 958–962.

Bernier, R., Golzio, C., Xiong, B., Stessman, H.A., Coe, B.P., Penn, O., Witherspoon, K., Gerdts, J., Baker, C., Vulto-van Silfhout, A.T., et al. (2014). Disruptive CHD8 mutations define a subtype of autism early in development. Cell *158*, 263–276.

Cotney, J., Muhle, R.A., Sanders, S.J., Liu, L., Willsey, A.J., Niu, W., Liu, W., Klei, L., Lei, J., Yin, J., et al. (2015). The autism-associated chromatin modifier CHD8 regulates other autism risk genes during human neurodevelopment. Nat. Commun. *6*, 6404.

Curtin, C., Anderson, S.E., Must, A., and Bandini, L. (2010). The prevalence of obesity in children with autism: a secondary data analysis using nationally representative data from the National Survey of Children's Health. BMC Pediatr. *10*, 11.

Curtin, C., Jojic, M., and Bandini, L.G. (2014). Obesity in children with autism spectrum disorder. Harv. Rev. Psychiatry *22*, 93–103.

Egan, C.M., Nyman, U., Skotte, J., Streubel, G., Turner, S., O'Connell, D.J., Rraklli, V., Dolan, M.J., Chadderton, N., Hansen, K., et al. (2013). CHD5 is required for neurogenesis and has a dual role in facilitating gene expression and polycomb gene repression. Dev. Cell *26*, 223–236.

Feng, W., Khan, M.A., Bellvis, P., Zhu, Z., Bernhardt, O., Herold-Mende, C., and Liu, H.K. (2013). The chromatin remodeler CHD7 regulates adult neurogenesis via activation of SoxC transcription factors. Cell Stem Cell *13*, 62–72.

Gaspar-Maia, A., Alajem, A., Polesso, F., Sridharan, R., Mason, M.J., Heidersbach, A., Ramalho-Santos, J., McManus, M.T., Plath, K., Meshorer, E., and Ramalho-Santos, M. (2009). Chd1 regulates open chromatin and pluripotency of embryonic stem cells. Nature *460*, 863–868.

Guo, H., Ma, O., Speck, N.A., and Friedman, A.D. (2012). Runx1 deletion or dominant inhibition reduces Cebpa transcription via conserved promoter and distal enhancer sites to favor monopoiesis over granulopoiesis. Blood *119*, 4408–4418.

Hall, J.A., and Georgel, P.T. (2007). CHD proteins: a diverse family with strong ties. Biochem. Cell Biol. *85*, 463–476.

Ho, L., and Crabtree, G.R. (2010). Chromatin remodelling during development. Nature *463*, 474–484.

Ishihara, K., Oshimura, M., and Nakao, M. (2006). CTCF-dependent chromatin insulator is linked to epigenetic remodeling. Mol. Cell *23*, 733–742.

Katayama, Y., Nishiyama, M., Shoji, H., Ohkawa, Y., Kawamura, A., Sato, T., Suyama, M., Takumi, T., Miyakawa, T., and Nakayama, K.I. (2016). CHD8 haploinsufficiency results in autistic-like phenotypes in mice. Nature *537*, 675–679.

Kita, Y., Nishiyama, M., and Nakayama, K.I. (2012). Identification of $CHD7_S$ as a novel splicing variant of CHD7 with functions similar and antagonistic to those of the full-length $CHD7_L$. Genes Cells *17*, 536–547.

Krueger, K.C., Costa, M.J., Du, H., and Feldman, B.J. (2014). Characterization of Cre recombinase activity for in vivo targeting of adipocyte precursor cells. Stem Cell Reports *3*, 1147–1158.

Marfella, C.G., and Imbalzano, A.N. (2007). The Chd family of chromatin remodelers. Mutat. Res. *618*, 30–40.

Muir, L.A., Neeley, C.K., Meyer, K.A., Baker, N.A., Brosius, A.M., Washabaugh, A.R., Varban, O.A., Finks, J.F., Zamarron, B.F., Flesher, C.G., et al. (2016). Adipose tissue fibrosis, hypertrophy, and hyperplasia: Correlations with diabetes in human obesity. Obesity (Silver Spring) *24*, 597–605.

Neale, B.M., Kou, Y., Liu, L., Ma'ayan, A., Samocha, K.E., Sabo, A., Lin, C.F., Stevens, C., Wang, L.S., Makarov, V., et al. (2012). Patterns and rates of exonic *de novo* mutations in autism spectrum disorders. Nature *485*, 242–245.

Nishiyama, M., Oshikawa, K., Tsukada, Y., Nakagawa, T., Iemura, S., Natsume, T., Fan, Y., Kikuchi, A., Skoultchi, A.I., and Nakayama, K.I. (2009). CHD8 suppresses p53-mediated apoptosis through histone H1 recruitment during early embryogenesis. Nat. Cell Biol. *11*, 172–182.

Nishiyama, M., Skoultchi, A.I., and Nakayama, K.I. (2012). Histone H1 recruitment by CHD8 is essential for suppression of the Wnt-β-catenin signaling pathway. Mol. Cell. Biol. *32*, 501–512.

O'Roak, B.J., Vives, L., Fu, W., Egertson, J.D., Stanaway, I.B., Phelps, I.G., Carvill, G., Kumar, A., Lee, C., Ankenman, K., et al. (2012a). Multiplex targeted sequencing identifies recurrently mutated genes in autism spectrum disorders. Science *338*, 1619–1622.

O'Roak, B.J., Vives, L., Girirajan, S., Karakoc, E., Krumm, N., Coe, B.P., Levy, R., Ko, A., Lee, C., Smith, J.D., et al. (2012b). Sporadic autism exomes reveal a highly interconnected protein network of *de novo* mutations. Nature *485*, 246–250.

Odawara, J., Harada, A., Yoshimi, T., Maehara, K., Tachibana, T., Okada, S., Akashi, K., and Ohkawa, Y. (2011). The classification of mRNA expression levels by the phosphorylation state of RNAPII CTD based on a combined genome-wide approach. BMC Genomics *12*, 516.

Rosen, E.D., and MacDougald, O.A. (2006). Adipocyte differentiation from the inside out. Nat. Rev. Mol. Cell Biol. *7*, 885–896.

Rosen, E.D., and Spiegelman, B.M. (2006). Adipocytes as regulators of energy balance and glucose homeostasis. Nature *444*, 847–853.

Sakamoto, I., Kishida, S., Fukui, A., Kishida, M., Yamamoto, H., Hino, S., Michiue, T., Takada, S., Asashima, M., and Kikuchi, A. (2000). A novel β-catenin-binding protein inhibits β-catenin-dependent Tcf activation and axis formation. J. Biol. Chem. *275*, 32871–32878.

Sanchez-Gurmaches, J., Hsiao, W.Y., and Guertin, D.A. (2015). Highly selective in vivo labeling of subcutaneous white adipocyte precursors with Prx1-Cre. Stem Cell Reports *4*, 541–550.

Schaaf, C.P., and Zoghbi, H.Y. (2011). Solving the autism puzzle a few pieces at a time. Neuron *70*, 806–808.

Siersbæk, R., Nielsen, R., John, Gormley et, Sung, M.H., Baek, S., Loft, A., Hager, G.L., and Mandrup, S. (2011). Extensive chromatin remodeling and establishment of transcription factor 'hotspots' during early adipogenesis. EMBO J. *30*, 1459–1472.

Siersbæk, R., Nielsen, R., and Mandrup, S. (2012). Transcriptional networks and chromatin remodeling controlling adipogenesis. Trends Endocrinol. Metab. *23*, 56–64.

Siersbæk, R., Rabiee, A., Nielsen, R., Sidoli, S., Traynor, S., Loft, A., Poulsen, L.C., Rogowska-Wrzesinska, A., Jensen, O.N., and Mandrup, S. (2014). Transcription factor cooperativity in early adipogenic hotspots and super-enhancers. Cell Rep. *7*, 1443–1455.

Siersbaek, R., Madsen, J.G.S., Javierre, B.M., Nielsen, R., Bagge, E.K., Cairns, J., Wingett, S.W., Traynor, S., Spivakov, M., Fraser, P., et al. (2017). Dynamic rewiring of promoter-anchored chromatin loops during adipocyte differentiation. Mol. Cell *66*, 420–435.

Simon, J.M., Giresi, P.G., Davis, I.J., and Lieb, J.D. (2012). Using formaldehyde-assisted isolation of regulatory elements (FAIRE) to isolate active regulatory DNA. Nat. Protoc. *7*, 256–267.

Stephens, J.M. (2012). The fat controller: adipocyte development. PLoS Biol. *10*, e1001436.

Sugathan, A., Biagioli, M., Golzio, C., Erdin, S., Blumenthal, I., Manavalan, P., Ragavendran, A., Brand, H., Lucente, D., Miles, J., et al. (2014). CHD8 regulates neurodevelopmental pathways associated with autism spectrum disorder in neural progenitors. Proc. Natl. Acad. Sci. USA *111*, E4468–E4477.

Talkowski, M.E., Rosenfeld, J.A., Blumenthal, I., Pillalamarri, V., Chiang, C., Heilbut, A., Ernst, C., Hanscom, C., Rossin, E., Lindgren, A.M., et al. (2012). Sequencing chromosomal abnormalities reveals neurodevelopmental loci that confer risk across diagnostic boundaries. Cell *149*, 525–537.

Taylor, B., Jick, H., and Maclaughlin, D. (2013). Prevalence and incidence rates of autism in the UK: time trend from 2004-2010 in children aged 8 years. BMJ Open *3*, e003219.

Vissers, L.E., van Ravenswaaij, C.M., Admiraal, R., Hurst, J.A., de Vries, B.B., Janssen, I.M., van der Vliet, W.A., Huys, E.H., de Jong, P.J., Hamel, B.C., et al. (2004). Mutations in a new member of the chromodomain gene family cause CHARGE syndrome. Nat. Genet. *36*, 955–957.

Wang, L., Xu, S., Lee, J.E., Baldridge, A., Grullon, S., Peng, W., and Ge, K. (2013). Histone H3K9 methyltransferase G9a represses PPARγ expression and adipogenesis. EMBO J. *32*, 45–59.

Zheng, Z., Zhang, L., Li, S., Zhao, F., Wang, Y., Huang, L., Huang, J., Zou, R., Qu, Y., and Mu, D. (2017). Association among obesity, overweight and autism spectrum disorder: a systematic review and meta-analysis. Sci. Rep. *7*, 11697.

Cell Reports, Volume *23*

Supplemental Information

The Autism-Related Protein CHD8 Cooperates with C/EBPβ to Regulate Adipogenesis

Yasuyuki Kita, Yuta Katayama, Taichi Shiraishi, Takeru Oka, Tetsuya Sato, Mikita Suyama, Yasuyuki Ohkawa, Keishi Miyata, Yuichi Oike, Michiko Shirane, Masaaki Nishiyama, and Keiichi I. Nakayama

SUPPLEMENTAL FIGURES

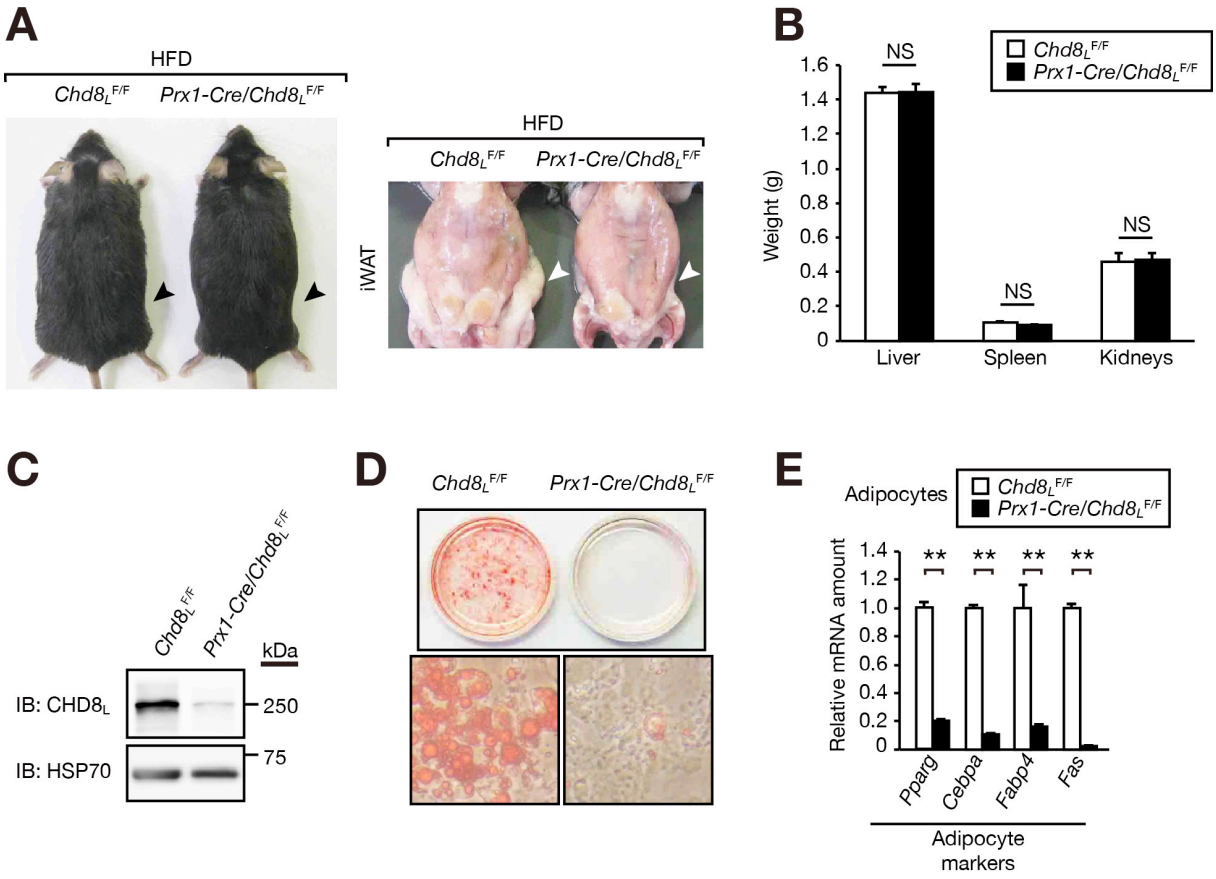

Figure S1. Ablation of *Chd8* in Preadipocytes Reduces iWAT Mass. Related to Figure 6

(A) Gross appearance of HFD-fed *Chd8*$_L^{F/F}$ and *Prx1-Cre/Chd8*$_L^{F/F}$ mice at 15 weeks of age. Arrowheads indicate iWAT.

(B) Weight of liver, spleen, and kidneys for HFD-fed *Chd8*$_L^{F/F}$ and *Prx1-Cre/Chd8*$_L^{F/F}$ mice at 15 weeks of age. NS by Student's *t* test.

(C and D) Preadipocytes isolated from iWAT of *Chd8*$_L^{F/F}$ and *Prx1-Cre/Chd8*$_L^{F/F}$ mice were subjected to immunoblot analysis of CHD8 (C) or were induced to undergo adipogenesis for 8 days and then stained with oil red O (D).

(E) Quantitative RT-PCR analysis of adipogenic gene expression in *Chd8*$_L^{F/F}$ or *Prx1-Cre/Chd8*$_L^{F/F}$ preadipocytes induced to differentiate for 8 days. Data are means ± SD (*n* = 6 independent experiments). $^{**}P < 0.01$ (Student's *t* test).

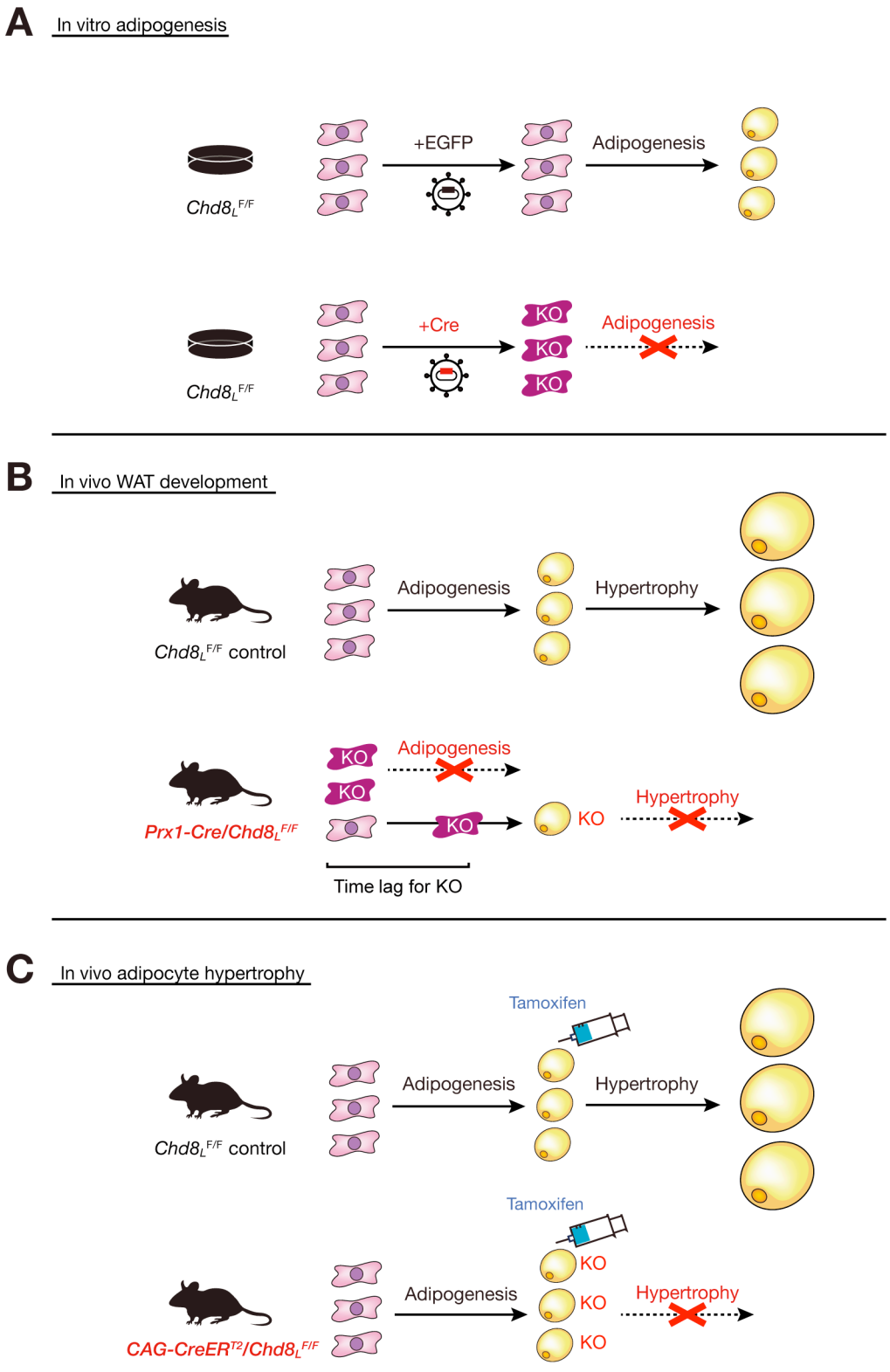

Figure S2. Summary of CHD8 Knockout Phenotypes. Related to Discussion

(A) The efficiency of retrovirus-mediated Cre expression in *Chd8*$_L^{F/F}$ preadipocytes in vitro is almost 100%, with the resulting knockout (KO) of CHD8$_L$ leading to a total block of adipogenesis.

(B) Expression of *Cre* under the control of the *Prx1* promoter is not complete during adipogenesis in vivo, with the result that some cells undergo delayed deletion of $Chd8_L$ after adipogenesis and then show a defect in adipocyte hypertrophy.
(C) Expression of *Cre* under the control of the CAG promoter in mature adipocytes reveals that deletion of $Chd8_L$ results in a defect in adipocyte hypertrophy.

SUPPLEMENTAL TABLES

Table S1. Primer sequences (5'→3') for RT-PCR analysis. Related to Experimental Procedures

Gene	Forward primer	Reverse primer
Arbp	GAGGAATCAGATGAGGATATGGGA	AAGCAGGCTGACTTGGTTGC
Cebpa	CAAGAACAGCAACGAGTACCG	GTCACTCGTCAACTCCAGCAC
Cebpb	CTATTTCTATGAGAAAAGAGGCGTATGTAT	ATTCTCCCAAAAAAGTTTATTAAAATGTCT
Cebpd	TGCCCACCCTAGAGCTGTG	CGCTTTGTGGTTGCTGTTGA
Chd8L	CTGGCTGATGAAATGGGATT	TAATGGTGGACAATGGAGCA
Fabp4	AAGGTGAAGAGCATCATAACCCT	TCACGCCTTTCATAACACATTCC
Fas	TTCCGTCACTTCCAGTTAGAG	TTCAGTGAGGCGTAGTAGACA
Glut4	GTGACTGGAACACTGGTCCTA	CCAGCCACGTTGCATTGTAG
Krox20	TTGACCAGATGAACGGAGTG	CCAGAGAGGAGGTGGAAGTG
Pparg1	TGAAAGAAGCGGTGAACCACTG	TGGCATCTCTGTGTCAACCATG
Pparg1+2	GATGGAAGACCACTCGCATT	AACCATTGGGTCAGCTCTTG
Pref1	GACCCACCCTGTGACCCC	CAGGCAGCTCGTGCACCCC

Table S2. Primer sequences (5'→3') for ChIP and FAIRE analyses. Related to Experimental Procedures

Gene	Forward primer	Reverse primer
Cebpa (-2 kb)	AACCCCTGGGTGTTTAGAGC	GGTTGAAGGAAGCTGGAACA
Cebpa (-1.5 kb)	TAGAGAAGCTGGGCGAAAGA	AGGTTGGAGACTGCTTTGGA
Cebpa (-1 kb)	CGCTCTCCTTAGGGTCCTTT	TCTTTTTCATTGCGTCTCCA
Cebpa (-0.1 kb)	CATGCCGGGAGAACTCTAAC	CTCTGGAGGTGACTGCTCATC
Cebpa (+0.2 kb)	ACATCAGCGCCTACATCGAC	TCCCGGGTAGTCAAAGTCAC
Cebpa (+36 kb)	GAAATGGGGGAGGTTTCATT	GACACACCCTGTCCCTCTGT
Cebpa (+37 kb)	AACAGGAAAGATGGCACCAG	CCACACCCCTCTATGTGATG
Cebpa (+37.5 kb)	AAGCCAGACCCTTACCACCT	CTAGCCAAACCCTGCTTCTG
Pparg1 (-0.75 kb)	AACTGTCTATCATGTGGGCTTCAG	GAGGGCCTGAGAATCTCTTGTTT
Pparg1 (-0.1 kb)	TGAGGGACACGGGACCTT	CCGTGCGCTGGTTACCT
Pparg1 (+0.5 kb)	GGATCTGACTGGCTAGGTGACT	GCAGCCCTGTCAGAATGTGA
Pparg1 (+1.5 kb)	GCCCCATCGTCATCACGTT	CAGACCATCCTGATGTGTAAGAA
Pparg2 (-0.3 kb)	CCCTCACAGAACAGTGAATGTGT	TGCTTTGGCAAGACTTGGTACAT
Pparg2 (+0.5 kb)	GCTTCCTCTCTTATTGTGTTAGATATCTTTCA	TCAAAGTAAAATAAAAAATGCCTGAAGAAGAACA
Pparg2 (+97 kb)	TCCTACTCCAAGGCCACAAC	CCTGTGGCAACTGATGTTTG
Pparg2 (+97.5 kb)	GCTGTGGTGAAACGACAGTTATTAG	CTTGGGAGCTACAGCCTTGTG
Pparg2 (+98.5 kb)	GGTGTCAGATCCCTTGCAGT	CTGCTCTTGTGGAACACCTG
Runx2	GTGTGAATGCTTCATTCGCCT	ACCGCACTTGTGGTTCTGTG